DOI: 10.1021/ma902588j

Macromolecules
ARTICLE

Swelling Study of Responsive Polyelectrolyte Brushes Grafted from Mica Substrates: Effect of pH, Salt, and Grafting Density

Béatrice Lego,[†] W. G. Skene,*[,†] and Suzanne Giasson*[,†,‡]

[†]*Department of Chemistry and* [‡]*Faculty of Pharmacy, Centre for Self-Assembled Chemical Structures, Université de Montréal, C.P. 6128, succursale Centre-Ville, Montréal, QC, Canada H3C 3J7*

Received November 26, 2009; Revised Manuscript Received March 9, 2010

ABSTRACT: Poly(acrylic acid) (PAA) brushes covalently linked to mica were prepared using the *graft from* approach in a two-step process: (i) poly(*tert*-butyl acrylate) (P*t*BA) brushes were first synthesized by atom transfer radical polymerization directly from an activated mica substrate (ii) followed by hydrolysis to generate PAA brushes. The hydrolysis reaction was confirmed by water contact angle measurements, polymer thickness measurements, and FTIR. The swelling behavior of the brushes in aqueous solutions was measured by examining the change in brush thickness (L), using atomic force microscopy (AFM), as a function of polymer grafting density (σ), pH, and salt (NaCl) concentration (C_s). A sharp transition from collapsed to stretched conformation was found at pH 7.5. For pH $\leq$ 7, the acrylic acid groups are not dissociated, and no swelling of the polymer layer was observed relative to the dry state, regardless of grafting density and salt concentration. For pH $\geq$ 7.5, the brushes behaved as charged polymer brushes exhibiting Pincus and salted-brush regimes that were dependent on the salt concentration. In salt-free solution, the equilibrium thickness scales with surface grafting density according to $L \propto \sigma^{0.87}$, and at high salt concentrations, the brushes collapse according to $L \propto \sigma^{1.09} C_s^{-0.17}$. The swelling behavior of PAA brushes was reversible with changes in pH and salt concentration under the studied experimental conditions.

Introduction

The control of surface properties using end-grafted polymers or polymer brushes represents an important scientific issue for developing responsive surfaces such as biocompatible substrates for impeding nonspecific adsorption of macromolecules, surfaces exhibiting switchable wettability, and self-lubricating surfaces, to name but a few. Surface properties of polymer-coated surfaces are dependent on the chemical composition of the outermost surface layer and more particularly on the polymer conformation. For example, the conformation adopted by polymer chains stretched along the normal direction to the grafting surface, referred to as a polymer brush, is different from typically flexible polymer chains in solution that adopt random-walk configurations. The specific brush conformation controls surface properties such as autophobicity,[1−3] lubricity,[4−9] and antifouling,[10−13] among others. Given their sensitivity to environmental conditions, end-grafted polymers can be used for modifying surface properties in a controlled and reversible manner via changes in their conformation associated with changes in their surroundings. Weak polyelectrolyte (PE) brushes, also called annealed brushes, represent interesting systems because the degree of dissociation of the chains can be varied via changes in pH and ionic strength, resulting in another parameter for reversibly tuning the polymer conformation. On the other hand, strong PE brushes have a degree of dissociation that is independent of pH and ionic strength and are therefore called quenched brushes.

A common and practical means for probing changes in brush conformation is by measuring the swelling of the brush with changes in environmental conditions (i.e., ionic strength and pH). Theoretical studies of polyelectrolyte brushes predict a complex swelling behavior depending on the degree of dissociation of the chain (α), grafting density (σ), and concentration of added salt (C_s).[14−19] Different regimes have been proposed to describe the variation in brush height or brush thickness (L) as a function of these parameters. For relatively dense and charged brushes in the absence of added salt, three different regimes, based on simple scaling description, are often used: (i) weakly charged brushes behaving as quasi-neutral brushes (neutral brush regime) with $L \propto N\sigma^{1/3}$, where N is the number of repeating units of the polymer chain, (ii) charged brushes with all the counterions located within the brush whose thickness is mainly controlled by the osmotic pressure of the counterions (osmotic brush regime) and independent of σ ($L \propto N\alpha^{1/2}$), and (iii) charged brushes with the counterion distribution extending beyond the brush (Pincus regime) and whose behavior is mainly controlled by the electrostatic repulsion between units ($L \propto N^3\sigma\alpha^2$). The presence of added electrolytes affects the electrostatic interactions within and between the chains as well as the osmotic pressure of the counterions. As a consequence, the swelling behavior can be strongly influenced by the presence of added salt. For instance, for annealed PE brushes at high grafting density and low salt concentrations, the brush thickness is expected to depend on the grafting density and the salt concentration according to:[14]

$$L \propto N\sigma^{-1/3}\left(\frac{\alpha_b}{1-\alpha_b}C_{H^+} + C_s\right)^{1/3}$$

where α_b is the degree of dissociation of the isolated chains in solution. This regime is generally referred to as the annealed osmotic regime. For salt concentrations larger than the concentration of the brush counterions, electrostatic screening effects are expected to reduce the brush thickness according to $L \propto N\sigma^{1/3}\alpha^{2/3}C_s^{-1/3}$.[14] This regime is called salted brush regime.

Most experimental studies of weak polyacid brushes focus on PAA and its derivatives grafted on silica substrates and report the variation of the brush thickness as a function of pH, salt concentration, and grafting density.[20−26] These studies agree

*To whom correspondence should be addressed. E-mail: suzanne.giasson@umontreal.ca (S.G.) or w.skene@umontreal.ca (W.G.S.).

 Published on Web 04/12/2010

only qualitatively with the predicted theory of charged brushes in that weak polyelectrolyte brushes show an expected nonmonotonic behavior as a function of salt concentration.[20−24,26] It has been shown that the brush thickness initially increases with increasing salt concentration, which corresponds to the annealed osmotic regime, and subsequently decreases with increasing salt concentration in the salted brush regime.[20,21,23,24,26] Most of these studies show a weaker effect of salt concentration on the brush thickness than the theoretically predicted one for the annealed osmotic brush regime[14] with different scaling laws ($L \propto C_s^{0}$ to $L \propto C_s^{0.3}$).[20,21,23−26] Although discrepancies between results of various studies are assumed to originate from different grafting densities, this has not been demonstrated. Despite the numerously reported experimental studies of end-grafted polyelectrolyte brushes, to the best of our knowledge, only one quantitatively correlates the brush thickness as a function of grafting density and salt concentration.[26] The lack of experimental−theoretical correlation concomitant with inconsistent experimental data illustrate the complex swelling behavior of weak polyelectrolyte brushes. As a result, there is a need to better control the parameters affecting brush swelling, in particular the grafting density and electrostatic interactions, in order to establish reliable structure/properties correlations.

Herein we examine the behavior of end-grafted PAA layers covalently attached to mica substrates in order to better understand the reversible swelling behavior of charged polymer brushes. Grafting densities covering an order of magnitude were investigated for elucidating the behavior of end-grafted polyelectrolytes across different surface coverage regimes. This is important given the inconsistencies of previous works that examined limited grafting densities. The role of electrostatic charges on the swelling behavior of PAA was also examined by varying the degree of dissociation of the chains with changes in pH and ionic strength. While previous studies focused on neutral and acid pH, we herein examine the swelling effect with pH ranging from 6 to 9 for verifying the scaling relations for charged brushes under different degrees of polymer dissociation. The thickness of the PAA layer as a function of grafting density, pH, and salt concentration is measured in solution using the AFM step-height method. A better understanding of the complex responsive behavior of weak polyelectrolyte brushes is highlighted while bringing new experimental support to theoretical models.

Experimental Section

General Methods and Materials. Chemicals were purchased from Aldrich unless otherwise stated. Granular anhydrous sodium chloride (NaCl, 99.999%), tris(hydroxymethyl)aminomethane (Trizma base, 99.9%), and trifluoroacetic acid (TFA, 99%) were used as received. Milli-Q quality water was obtained from a Millipore Gradient A 10 purification system (resistance 18.2 MΩ·cm, TOC 4 ppb). Methylene chloride (CH_2Cl_2) used for the hydrolysis reaction was filtered through a 0.2 μm PTFE membrane. Absolute ethanol used for cleaning was distilled prior to use. Ruby mica sheets were obtained from S & J Trading Inc. All surface manipulations were performed in a clean laminar airflow cabinet preventing dust deposition on the surfaces, and all glassware was carefully cleaned.

Surface Preparation and Polymer Hydrolysis. P*t*BA brushes on mica surfaces were synthesized as previously reported.[27] More information on monomer purification and on the initiator grafting reaction is available in the Supporting Information. All surface samples were synthesized with a targeted molecular weight in solution of 52 ± 3 kg/mol, and it was assumed that the brush molecular weight was similar to that of the free polymer in solution. All samples were prepared according to the step-height method (see the Characterization Techniques section for more details). End-grafted PAA layers were obtained by hydrolysis of end-grafted P*t*BA layers as follows. End-grafted P*t*BA covalently attached to mica surfaces were immersed in 11 mL of CH_2Cl_2/TFA solution (10:1 v/v) at room temperature. The surfaces were left in the solution overnight with stirring. The mica sheets were then removed from the solution, washed for about 1 min under a gentle flow of absolute ethanol, Milli-Q water, and again with absolute ethanol, and then finally dried with a nitrogen gun for about 1−2 min. The samples were stored in a desiccator when not in use.

Swelling Study as a Function of pH and Salt Concentration. For the swelling study of the PAA layers, a buffer solution was used to obtain different solutions with stable pH. 0.1 M Trizma base buffer solution was prepared in Milli-Q water. The initial pH of the solution was 10.2−10.6. The pH was adjusted to the desired value (pH 7, 7.5, or 9) by adding a given volume of a 0.1 M HCl solution (1:1, 2:1, and 9:1 v/v pH 10 buffer solution/HCl, respectively). The ion concentration increases from 0.02 M to 0.1 M with the addition of HCl as pH decreases from 9 to 7. The solution at pH 6 was pure Milli-Q water. The pH of all solutions was measured with a Symphony SB20 pH meter (VWR Scientific Products) equipped with an Ag/AgCl electrode. The electrode was calibrated with pH 4.01, 7.00, and 10.01 buffer solutions. NaCl solutions were prepared either at pH 6 or pH 9. Samples were left in the given solution to equilibrate by stirring at least 2 h before being analyzed by AFM. Prior to AFM measurements, the pH of the buffer solutions and the salt solutions were verified and adjusted if necessary.

Characterization Techniques. Contact angle measurements were carried out using a FTA200 dynamic contact angle analyzer (First Ten Angstroms) with the sessile drop method. Data analyses were performed with the Fta32 Video software and using Milli-Q quality water as the probe liquid. Three separate measurements were done for each substrate, and the angle data were statistically combined. The variation around the mean contact angle averaged over three measurements was ±2°. The equilibrium contact angle of a chemically heterogeneous surface, θ_{obs}, can be related to the fraction of the different chemical groups f in terms of the phenomenological Cassie−Baxter and the modified related equations:[28]

$$[1+\cos(\theta_{obs})]^2 = f_1[1+\cos(\theta_1)]^2 + f_2[1+\cos(\theta_2)]^2 \quad \text{with } f_1+f_2 = 1 \tag{1}$$

The water contact angle of a surface covered with a maximum number of hydrophobic small molecules, $f_1 = 1$, is assumed to be $\theta_1 = 90°$ as previously reported,[29,30] while the water contact angle against a surface containing only OH groups, $f_2 = 1$, is $\theta_2 = 0°$ as experimentally determined (data not shown).

AFM images and polymer film thickness measurements in air under about 20% humidity were acquired at room temperature using a Nanoscope IIIa, Extended controller, and a MultiMode microscope (Digital Instruments, Santa Barbara, CA). In air, intermittent contact imaging (i.e., "tapping mode" imaging) was performed at a scan rate of 1 Hz for topographic imaging and at a scan rate of 0.5 Hz for step-height measurements using silicon cantilevers (Arrow, Nanoworld) with a resonance frequency of ∼285 kHz and a spring constant of ∼42 N/m. Images were acquired with medium oscillation damping (16−25%). AFM imaging and polymer film thickness measurements in water were done at room temperature using a Nanoscope IIIa, Extended controller, and a Dimension 3100 microscope (Digital Instruments, Santa Barbara, CA) equipped with a custom-made fluid cell. In water, intermittent contact (tapping mode) was performed at a scan rate of 1 Hz for topographic imaging and at a scan rate of 0.5 Hz for step-height measurements using silicon cantilevers (Macrolevers E) with a resonance frequency of ∼6−10 kHz in liquid and a spring constant of ∼0.1 N/m. Images were

Table 1. Water Contact Angle and Film Thickness Prior to and after Hydrolysis

immobilized initiator layer		grafted polymer layer					
		PtBA				PAA	
θ_{water} (±2°)	f_1 (%)[a]	θ_{water} (±2°)	dry thickness (±1 nm)[b]	σ (chain/nm^2)[c]	s (nm)	θ_{water} (±2°)	dry thickness (±1 nm)[b]
35	23	75	3.3	0.04	5	16	2.3 ± 0.7
37	25	72	5	0.06	4.1	10	2.4 ± 0.7
38	27	83	7	0.08	3.5	7	4.3 ± 0.9
41	31		12	0.15	2.6	31	5
61	60	84	16	0.20	2.2	36	7
66	67	86	26	0.32	1.8	17	12
68	70	84	25	0.34	1.7		11
74	79	84	32	0.38	1.6	34	14
75	81	84	41	0.49	1.4	26	17

[a] Calculated from eq 1. [b] Measured by AFM in air using step-height method. [c] Calculated from eq 2. The average molecular weight M_n of the free PtBA polymer is 52 ± 3 kg/mol.

acquired with weak oscillation damping (5−10% of amplitude attenuation) in order to avoid film compression. Data analyses were performed using the NanoScope III software (version 5.30r3sr3). In the text, dry and wet film thicknesses refer to the thickness measured in air and in liquid media, respectively. Film thickness was determined using the step-height method as previously reported.[27,31] Briefly, a thin sheet of mica, playing the role of a mask, was removed from the substrate to leave a clean surface used as reference for the step-height measurement. An AFM image of a typical step used for the height measurement is shown in the Supporting Information (Figure S1). For each sample, the film thickness was measured at two different areas on each mica surface. For each measurement, two thickness values were determined using step-height analysis and bearing analysis. The reported values are mean thicknesses of the four values obtained on each surface. The surface roughness and the standard deviation were calculated for each measurement and the largest value was reported as the error. In the present study, the regimes of low ($\sigma < 0.1$ chain/nm^2), moderate ($0.1 \leq \sigma < 0.3$ chain/nm^2), and high grafting density ($\sigma \geq 0.3$ chain/nm^2) are represented by 3, 2, and 4 different mica substrates, respectively.

The grafting density σ of the PtBA layer was calculated from the dry polymer layer thickness d using:

$$\sigma = \frac{d\rho N_A}{M_n} \quad (2)$$

where ρ is the density of PtBA (1.047 g cm^{-3}),[32] N_A is the Avogadro's number, and M_n is the molecular weight of the grafted polymer chains which is assumed to be similar to that of the free polymer in solution. The molecular weight of the free polymer, relative to polystyrene standards, was determined by GPC.

Infrared reflection−absorption spectroscopy (IRRAS) spectra of the polymer films grown on a silicon wafer were recorded with p-polarized light at an incidence angle of 70° with respect to the surface normal using a Bruker Vertex 70 spectrometer. A total of 1024 scans were coadded for each spectrum at 4 cm^{-1} spectral resolution. A silicon wafer bearing a grafted PAA brush was incubated for about 15 min in water (pH 6) under stirring after which it was dried under a flow of nitrogen. The IRRAS spectrum was then recorded. The same silicon wafer was then immersed in a Trizma base buffer solution at pH 9 for about 15 min with stirring after which it was dried under a flow of nitrogen. The IRRAS spectrum was then recorded.

Results and Discussion

Synthesis of End-grafted PAA on Mica. The initiator-functionalized mica substrates with various surface coverage were prepared as previously reported.[27] The initiator surface coverage (f_1) was estimated from the water contact angle according to eq 1 and varied from 23 to 81% (Table 1). These surfaces were then used to polymerize PtBA via surface-initiated ATRP in the presence of free initiator.[27] The free PtBA was analyzed by GPC in THF giving a molecular weight of 52 ± 3 kg/mol, corresponding to a calculated PAA molecular weight of 30 kg/mol. The molecular weight of the grafted polymer could not be determined because of the very small amount of polymer generated. However, experimental studies report similar molecular weight (of the same order of magnitude) for the grafted and the free polymer chains grown by ATRP.[33−35] Therefore, it is assumed that the molecular weights of the free and grafted polymer chains are similar in our study. The grafting densities of the grafted PtBA were calculated from the molecular weight of the free polymer (M_n) and from the dry film thickness (d) according to eq 2 and varied between 0.04 and 0.5 chain/nm^2. The corresponding distances between grafting sites ($s = 1/\sigma^{1/2}$) range from 5 to 1.4 nm. For comparison, the approximate characteristic sizes of the linear homopolymer of 52 ± 3 kg/mol in solution are 100 nm for the length of a fully extended chain ($\approx aN$ where a is the characteristic dimension of each repeating unit, 0.25 nm, and N is the average number of repeating units of the PtBA chain, 406), 9 nm for the Flory radius (R_F) of a swollen coil ($R_F \approx aN^{0.6}$) and 2 nm for the radius of a collapsed coil ($R_F \approx aN^{0.33}$).[27] Therefore, the surface coverage of the neutral PtBA brushes correspond to the brush regime ($s < R_F$).

Scheme 1. Illustration of the Formation of Grafted PAA Film on Mica Substrates

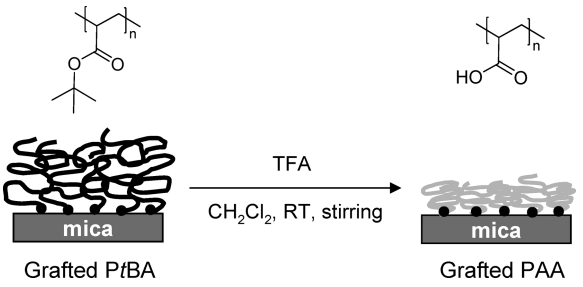

PtBA was converted to PAA by immersing the surface in CH_2Cl_2/TFA (10:1 v/v) at room temperature (Scheme 1). The hydrolysis of PtBA to PAA results in a decrease in both the water contact angle and film thickness (Table 1). The decrease in water contact angle confirms that a hydrophilic layer is obtained. A 50% decrease in film thickness upon converting PtBA to PAA is a result of losing the *tert*-butyl group giving rise to chain relaxation.[26,36,37] This is evidenced

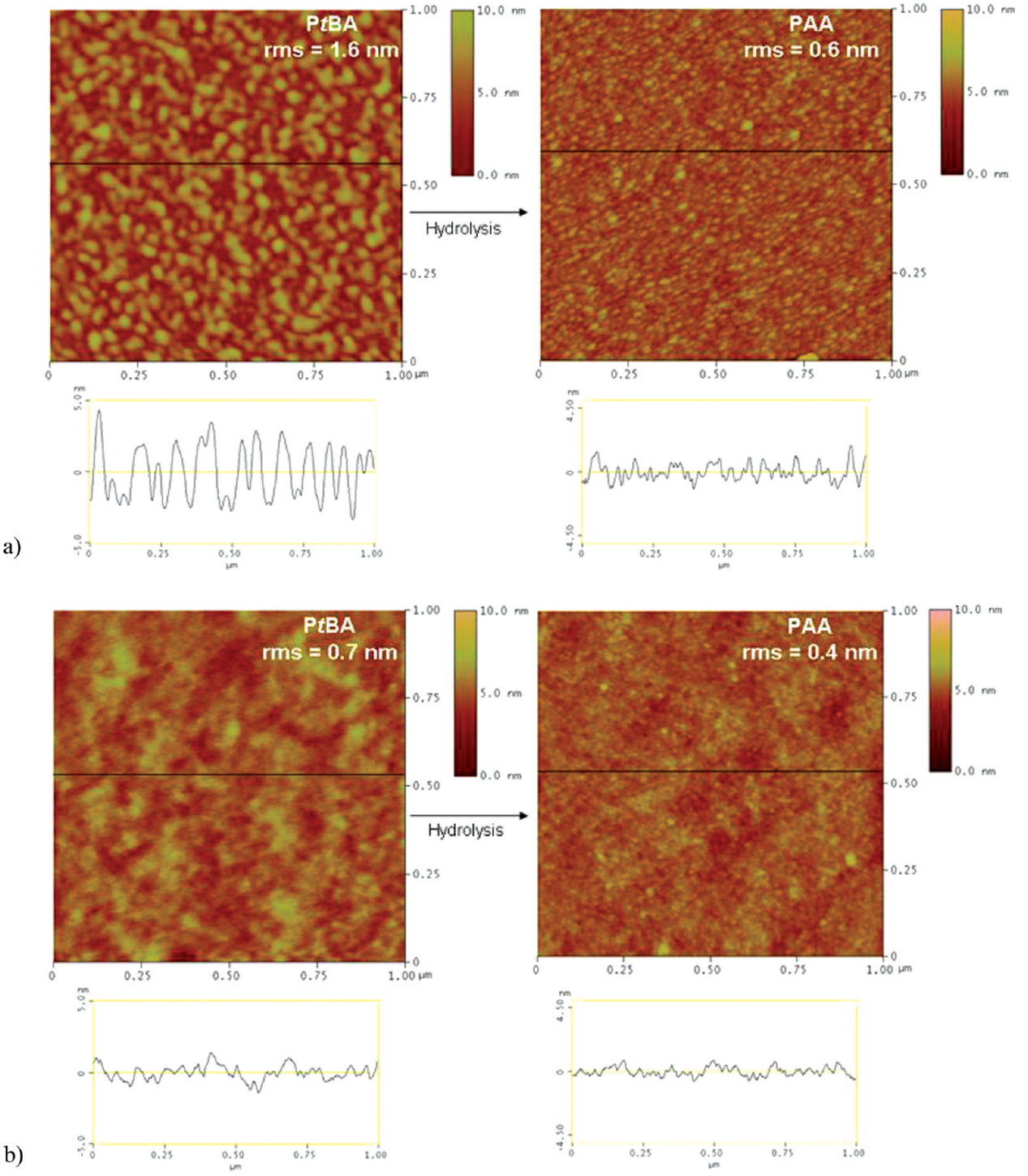

Figure 1. AFM and cross-section images in air of polymer films prior and after acid hydrolysis for two different grafting densities: (a) 0.04 chain/nm^2 and (b) 0.38 chain/nm^2. The cross sections corresponding to the black line shown in the AFM images are given below each image.

by AFM imaging where large aggregates are observed for the P*t*BA layer (Figure 1a). These reorganize into smaller and closely packed nodules upon hydrolyzing to PAA of low grafting density. However, such organization could not be clearly observed at high grafting density because the chains are closely packed and less mobile (Figure 1b). The change in film topography upon hydrolysis is associated with a decrease in the film roughness from 1.6 to 0.6 nm at low grafting density and from 0.7 to 0.4 nm at high grafting density. The conversion of P*t*BA to PAA brushes grafted from silicon wafers was confirmed by IRRAS. The IR spectrum of the PAA layer shows a broad carbonyl stretching band at 1728 cm^{-1} assigned to the carboxylic acid and no typical *tert*-butyl bending bands at 2980, 1393, and 1369 cm^{-1} (Figure 2a). The absence of these characteristic frequencies confirms that the protecting group was successfully cleaved and that the P*t*BA groups are converted to PAA.

The siloxane bond between the activated mica and the initiator along with the ester group connecting the initiator to the polymer are susceptible to hydrolysis leading to polymer cleavage.[26,38−40] To verify that such a cleavage

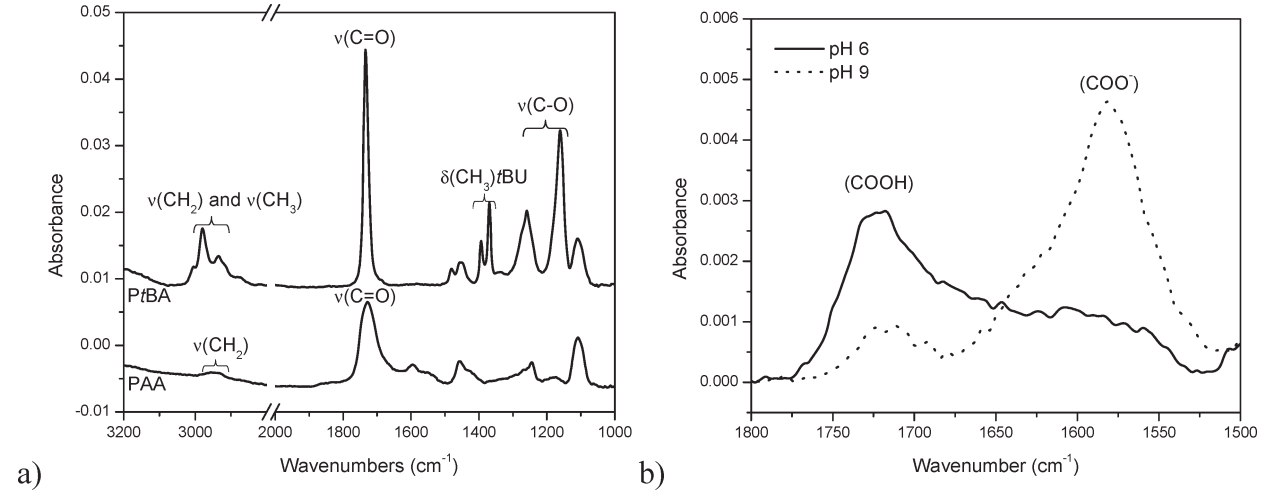

Figure 2. IRRAS spectra recorded in air: (a) P*t*BA film and PAA film chemically grafted on a silicon wafer; (b) PAA film grafted on a silicon wafer that were immersed in pH 6 (solid line) and pH 9 (dotted line) solutions for 15 min (only the carbonyl region is shown).

reaction did not occur under our hydrolysis conditions, we investigated the stability of the initiator layer and of the PAA layer under the same hydrolysis conditions. An initiator-functionalized mica substrate, with a water contact angle of 62 ± 2°, was immersed in CH_2Cl_2/TFA overnight, after which time the substrate was washed with ethanol and water. Water contact angle measured after immersion was 56 ± 2°, suggesting that the initiator layer is relatively stable under the hydrolysis condition. Therefore, chain cleavage due to initiator hydrolysis is considered negligible during the conversion of P*t*BA to PAA. Similarly, we studied the stability of the PAA layer by measuring the variation in PAA thickness at prolonged hydrolysis conditions. A mica substrate bearing a grafted PAA film with a thickness of 17 ± 2 nm was immersed in CH_2Cl_2/TFA for 3 days with stirring, after which time the substrate was thoroughly washed with a gentle flow of ethanol followed by rinsing with Milli-Q water. Thickness measurements by AFM revealed no significant change in the film thickness, confirming that polymer cleavage from the substrate does not occur under our hydrolysis conditions. This study confirms that the grafted layers are resistant to hydrolysis, and therefore, no chain cleavage occurs during P*t*BA conversion.

Swelling Study as a Function of pH and Grafting Density. The swelling behavior of PAA brushes was investigated by measuring the variation in polymer film thickness as a function of pH and the polymer grafting density. Both the dry and wet film thicknesses of the polymer were measured via AFM step-height measurements in air and water, respectively. The swelling behavior of the brushes was quantified using the swelling ratio (Q), defined as the ratio between the wet film thickness L and the dry film thickness d:

$$Q = \frac{L}{d} \tag{3}$$

The swelling ratio as a function of grafting density at different pH values is shown in Figure 3a. Q remains on the order of unity for pH 6 and 7, increases significantly at pH 7.5, and reaches a mean value of 10 at pH 9. The absence of brush swelling observed at pH < 7.5 suggests that the chains maintain the same collapsed conformation as that in the dry state. The morphology of a collapsed PAA layer in the dry state occurs as small aggregates that are also visible at pH 6 (Figure 4). These aggregates have a mean diameter of 10 nm. The height of a single aggregate cannot be determined by AFM as the aggregates form a dense and compact layer on the surface. The average dry thickness of the layers is reported in Table 1. The results confirm that the PAA layer is collapsed at pH 6, whereas the swollen PAA layer has a different morphology with no visible aggregates at pH 7.5 and pH 9 (Figure 4). The collapsed layer at pH 6 suggests that the PAA chains are protonated because of poor solvency of the undissociated PAA by water.[41−45] A significant increase in the swelling ratio was observed at pH 7.5 (Figure 3a). This is due to the presence of electrostatic repulsions within the brush resulting from dissociation of the PAA carboxylic acid groups, causing chain stretching. The dissociation of the PAA carboxylic acids with increasing pH was confirmed by IR. Figure 2b shows the IRRAS spectra of PAA grafted on a silicon wafer that was immersed in aqueous solutions of pH 6 and pH 9. The characteristic −COOH stretching at 1725 cm^{-1} is observed while that of COO^- at 1580 cm^{-1} is absent at pH 6. The PAA brushes therefore exist as undissociated brushes at pH 6. When the pH increases to pH 9, the ratio of the $COOH/COO^-$ stretching frequencies decreases, confirming that the acid groups along the polymer chains are dissociated.

The scaling relationship describing the swelling behavior of charged polymer brushes in good solvents predicts that the degree of dissociation (α) of weak polyacid decreases with increasing grafting density (σ) according to $\alpha \propto \sigma^{-1/3}$.[14] The pH transition between neutral and charged brushes at high grafting density is therefore expected to be higher than the acid dissociation constant of the acrylic acid monomer (pK_a = 4.25)[46] and of PAA in dilute solution (pK_a ∼ 4.2−5.5).[20,47,48] This has been experimentally shown with PAA brushes (M_n = 25 kg/mol) where the pK_a increases from 4 to 6 with increasing grafting density from 0.06 to 0.12 chain/nm^2.[20,49] Similarly, a pK_a of 6.8 for a PAA brush with a grafting density of 0.72 chain/nm^2 was reported.[25] Our results showing an abrupt increase in the swelling ratio at pH 7.5 suggest that the dissociation of the acid group occurs at pH 7.5, which is higher than the pK_a of the corresponding monomer (Figure 3a). This behavior is in contrast to a progressive transition that is usually observed with increasing pH.[20,25,49] In these previous studies, the PAA layers were swollen at the initial stage (pH 3) due to the brush preparation conditions. This suggests an initial dissociation of PAA acid groups and, therefore, a progressive dissociation with further increases in the pH of the solution. On the contrary, the PAA layers in our study are undissociated and remain

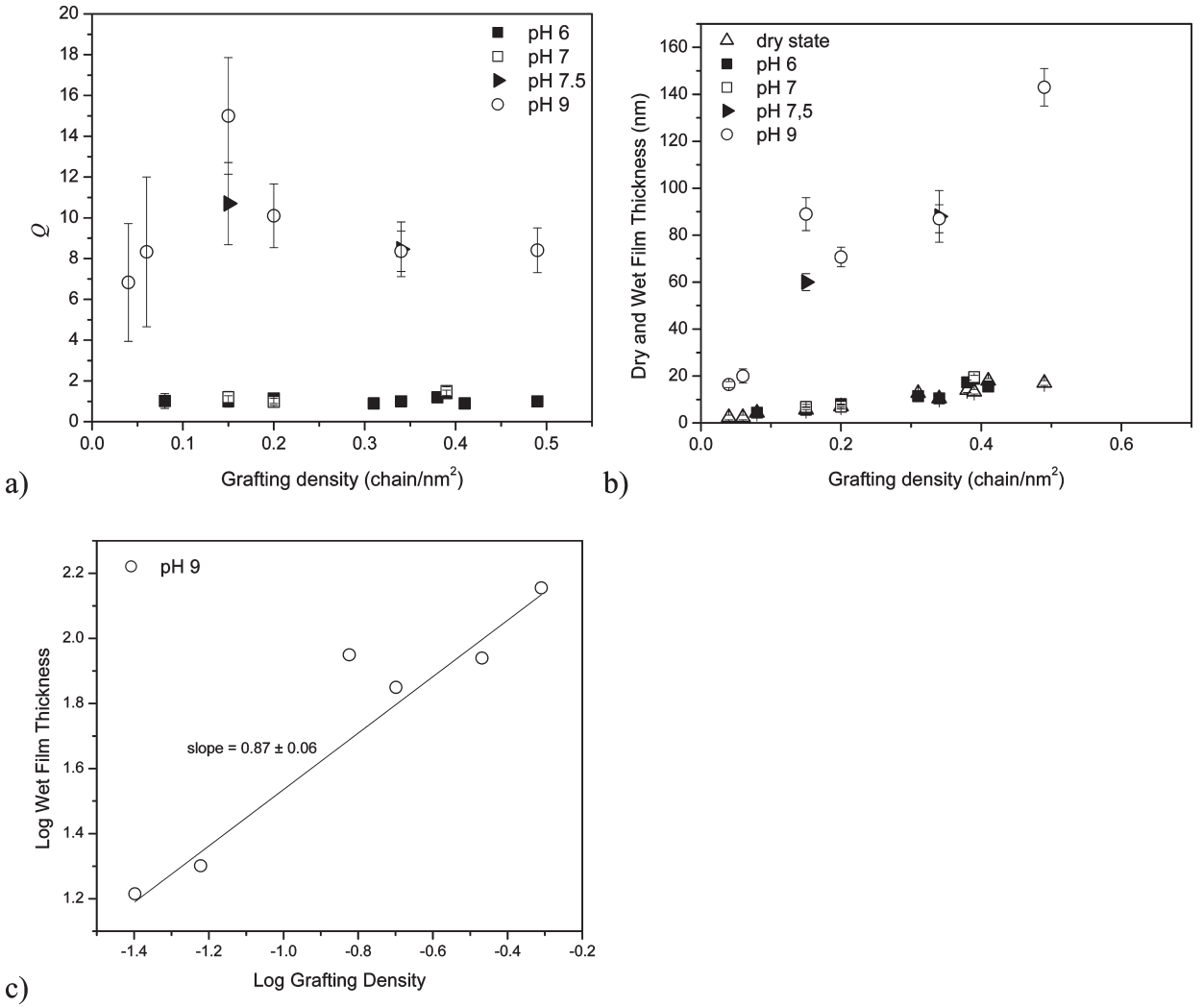

Figure 3. Swelling ratio (Q) and film thickness as a function of grafting density for different pH: dry state (opened triangles), pH 6 (solid squares), pH 7 (opened squares), pH 7.5 (closed triangles), and pH 9 (opened circles).

collapsed at pH $<$ 7.5 due to poor solvency. The increase in pH led to the dissociation of the PAA acid groups (Figure 2b) together with a better solubility of the charged PAA chains in water. The resulting sharp increase in Q with pH is similar to that observed with a change in solvent quality.[41,43] For pH $<$ 7.5 the change in ionic strength associated with the change in pH should not affect the brush swelling as the PAA are protonated (neutral brushes) (vide infra). The increase in ionic strength associated with the decrease in pH from 9 to 7.5 could induce a collapse of the brush. However, Q remains relatively insensitive to changes in ionic strength as shown in Figure 3a.

At pH $\geq$ 7.5, the measured film thickness is larger than that of a swollen coil ($\sim$9 nm) regardless of grafting density (Figure 3b). This confirms that the PAA polymer layer is in the brush regime for grafting densities ranging from 0.04 to 0.5 chain/nm^2. The maximum PAA layer thickness (i.e., ca. 140 nm at pH 9 and for large grafting density) is larger than the expected fully extended chain length of a 52 kg/mol P*t*BA chain of 406 repeating units (ca. 100 nm). This result suggests that the molecular weight of the grafted chains might be larger than the one of the free polymer in solution. An under-estimation of the grafted chain molecular weight would lead to a sur-estimation of the grafting density. However, an increase in the molecular weight of ca 21 kg/mol (based on the comparison of fully extended chain lengths 100 nm for 52 kg/mol and 140 nm for 73 kg/mol) would lead to an increase in the exponent of the scaling relationship L vs σ, of ca. 0.1 which does not significantly affect the interpretation of our results. The variation in the swelling ratio (Q) with pH for dissociated PAA brushes (pH $\geq$ 7.5) is independent of the grafting density within the experimental error (Figure 3a). The wet brush thickness increases with grafting density according to $L \propto \sigma^{0.87}$ at pH 9, as determined from the logarithmic representation of the experimental data (Figure 3b and 3c). The general trend of L increasing with σ has been qualitatively observed for PAA brushes.[20,26] However, to our knowledge, only one study reports a quantitative relationship between brush thickness and grafting density of $L \propto \sigma^{0.28}$ for PAA of M_n = 25 kg/mol at pH 5.8, in the absence of salt, and for grafting densities ranging from 0.08 to 0.8 chain/nm^2.[26] In this study, the degree of dissociation of the PAA brushes is assumed to be about 0.5 at pH 5.8.[26] Our results ($L \propto \sigma^{0.87}$) differ from that study and are closer to the charged brush behavior described by the Pincus regime ($L \propto \sigma$) than to the osmotic ($L \neq f(\sigma)$) or neutral ($L \propto \sigma^{1/3}$) regimes. This suggests that the PAA brushes are charged and that counterions are extending out of the brush. The slight deviation from the Pincus model can be explained by an under-estimation of the grafted chain molecular weight and/or by a nonhomogeneous distribution of charges along the brush and the size of the ions present in the buffer. The amine used to prepare the pH 9 buffer solution

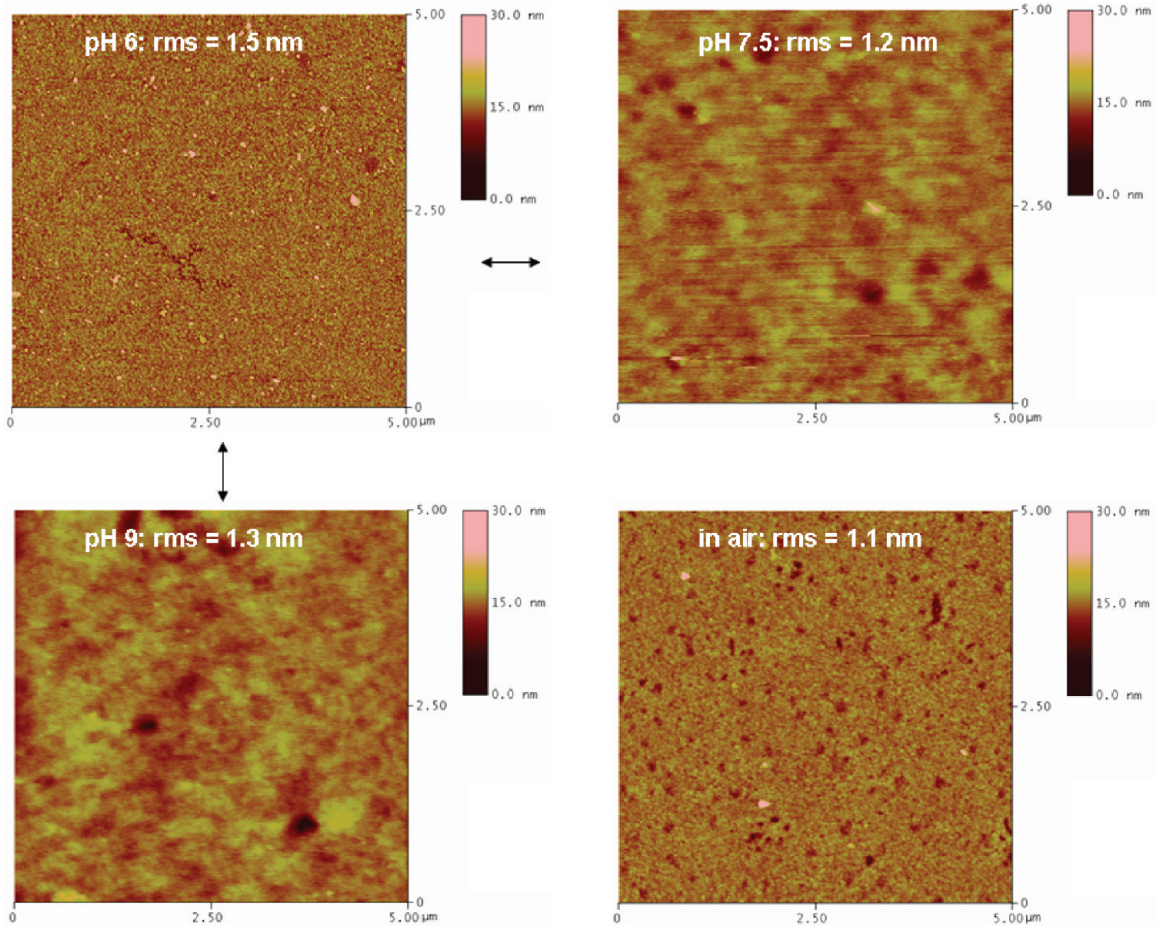

Figure 4. AFM images of a PAA brush with a grafting density of 0.34 chain/nm^2 exposed to different pH conditions. The AFM image of the layer in air is presented as a reference for the topography of a collapsed PAA layer.

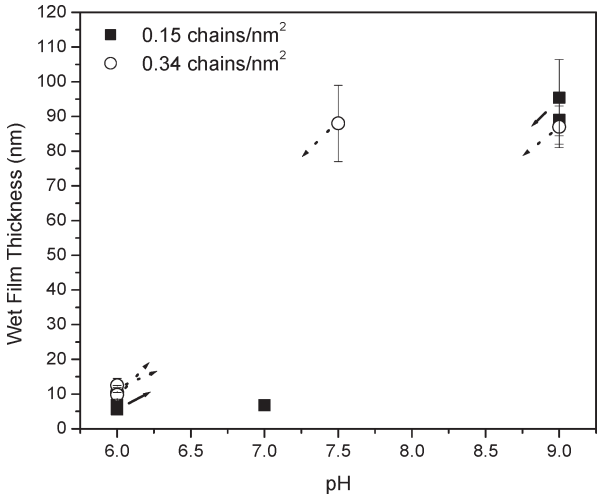

Figure 5. Reversibility of the PAA swelling behavior, as indicated by the arrows, for two grafting densities: 0.15 chain/nm^2 (solid squares) and 0.34 chain/nm^2 (open circles).

plays the role of counterions for the charged acid groups in the absence of added salt. Because of the large size of these counterions, the ions distribution might extend outside the brush. For the same reason, the dissociation of the PAA units at the water/brush interface might be favored compared to the dissociation at the brush/substrate interface. Meanwhile, the undissociated acids close to the surface protect the end-grafted initiator against unwanted hydrolysis (vide infra).

The reversible swelling behavior of PAA brushes as a function of pH was investigated for two samples: one at moderate (σ = 0.15 chains/nm^2) and another at high (σ = 0.34 chains/nm^2) grafting density (Figure 5). The samples were left to equilibrate for 2 h at a given pH, after which time the thickness of the layers was measured. The results show that the thickness increases at high pH and decreases reversibly to the initial thickness of that at pH 6 (Figure 5). The swelling of PAA layers is therefore reversible with polymer conformation, demonstrating that switching and tuning of surface properties in response to pH are possible.

The stability of the PAA layers exposed to pH 6 and 9 was also investigated. No significant change in wet film thickness ($\Delta L = 1.3 \pm 1$ nm) was observed for a PAA brush (σ = 0.15 chain/nm^2) immersed in water at pH 6 for a week. The stability of the PAA brush at pH 6 may be a result of the collapsed PAA layer that protects the immobilized initiator against hydrolysis. At pH 9, the PAA layer is ionized and swollen, exposing the labile initiator bonds to potential hydrolysis. To verify whether polymer cleavage occurred at this pH, a PAA brush (σ = 0.2 chain/nm^2) with an initial dry thickness of 7 ± 1 nm was left at pH 9 for different immersion times. No significant change in thickness was measured over 2 days ($\Delta L = 7 \pm 4$ nm), suggesting that the layer is stable and that no chain cleavage occurs during the given experimental time. This could be explained by the presence of undissociated repeating units close to the surface that act as a hydrophobic protective layer against hydrolysis.

Swelling Study as a Function of Salt Concentration and Grafting Density. The variation of the PAA layer thickness as

a function of added monovalent ions (NaCl) at pH 6 for different grafting densities was investigated (Figure 6). As previously shown, the PAA brushes are neutral ($\alpha \approx 0$) at pH 6. According to the theory of Zhulina et al.,[14,17,50] the degree of dissociation of annealed brushes is expected to increase with salt concentration, whereas α is expected to decrease with grafting density. However, our results show that the thickness of the PAA brushes is independent of salt concentration at pH 6 regardless of the grafting density (Figure 6). These results further contradict previous PAA studies of comparable grafting density that found an increase in the brush thickness with increasing salt concentration for $4 \leq$ pH ≤ 6.[20,26] This discrepancy could be associated with differences in the physical state of the PAA layers in the salt-free solution and/or the polymer molecular weight. In previous studies,[20] the PAA layers were swollen prior to the addition of salt. Therefore, as previously mentioned, some acid groups in the brush are dissociated prior to adjusting the pH and salt concentrations. Given that our PAA brushes are prepared in salt-free organic solution, the polymer remains undissociated and collapsed even when exposed to water at pH ≤ 7. Therefore, added ions cannot penetrate the collapsed hydrophobic brush at low pH. To verify whether or not the molecular weight of the grafted polymer is responsible for the observed discrepancies in the scaling laws with similar studies, the influence of the molecular weight on the brush swelling at pH 6 (Table 2) was investigated. The thicknesses measured at pH 6 and in the dry state are similar regardless of the polymer molecular weight. The PAA layer therefore remains undissociated even in water, and a pH > 7 is required to dissociate the acid groups. This is in contrast to its corresponding monomer whose pK_a is 4.25.

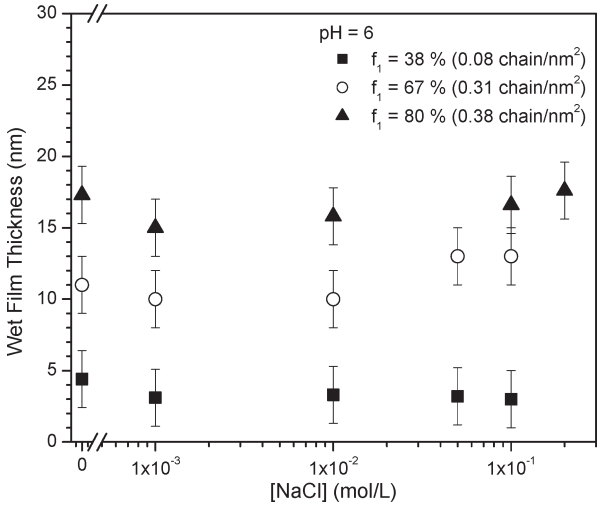

Figure 6. Wet film thickness of PAA layers at pH 6.0 as a function of salt concentration and grafting densities. The dry thicknesses were 4.3 nm (solid squares), 12 nm (opened circles), and 14 nm (solid triangles).

Table 2. Thickness in the Dry State and in Water at pH 6 for Different Molecular Weights of PAA Chains

immobilized initiator layer		PAA		
θ_{water} (±2°)	f_1 (%)	M_n (kg/mol)	dry thickness (±1 nm)	wet thickness in water at pH 6 (±1 nm)
72	76	2	3	5
72	76	12	6	6
73	78	25	14	17

The swelling behavior of PAA brush at pH 9 is significantly different from the one observed at pH 6. At pH 9, the dissociated polymer segments become sensitive to the ionic strength of the surrounding solution. The variation in the brush thickness as a function of the salt concentration at pH 9 is illustrated in Figure 7a for different grafting densities. For salt concentrations comprised between 0 and 1×10^{-3} M, the brush thickness seems to slightly increase compared to the one in a salt-free solution as expected for annealed polymer brushes at low salt concentrations and scales according to $L \propto \sigma^{0.96}$ (Figure 7a). The increase in the brush thickness might result from the dissociation of acid groups favored by the added salt and an increase in the osmotic pressure inside the brush due to the presence of small counterions such as Na^+.[14] For higher salt concentrations ($C_s \geq 1 \times 10^{-2}$ M), the brush thickness decreases with increasing salt concentration for all grafting densities (Figure 7a). The dependence of the brush height with

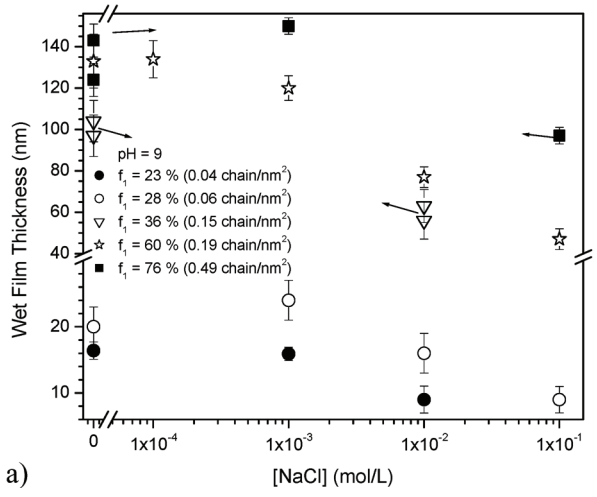

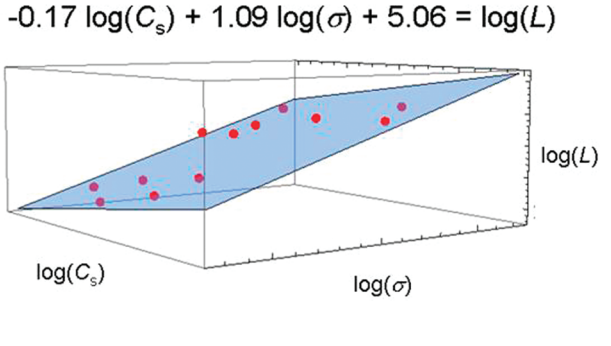

Figure 7. Swelling behavior of PAA layers with various grafting densities as a function of salt concentration at pH 9.0: (a) Wet film thickness of the PAA layers (the dry thicknesses were 2.3 nm (solid circles), 2.5 nm (opened circles), 5.6 nm (opened triangles), 5.5 nm (opened stars), and 17 nm (solid squares); the arrows indicate samples used for the reversibility study). (b) Wet film thickness versus salt concentration and grafting density plotted logarithmically for the salted brush regime (above 1×10^{-3} M). The experimental law of the brush height obtained by least-squares fit is $L \propto \sigma^{1.09} C_s^{-0.17}$.

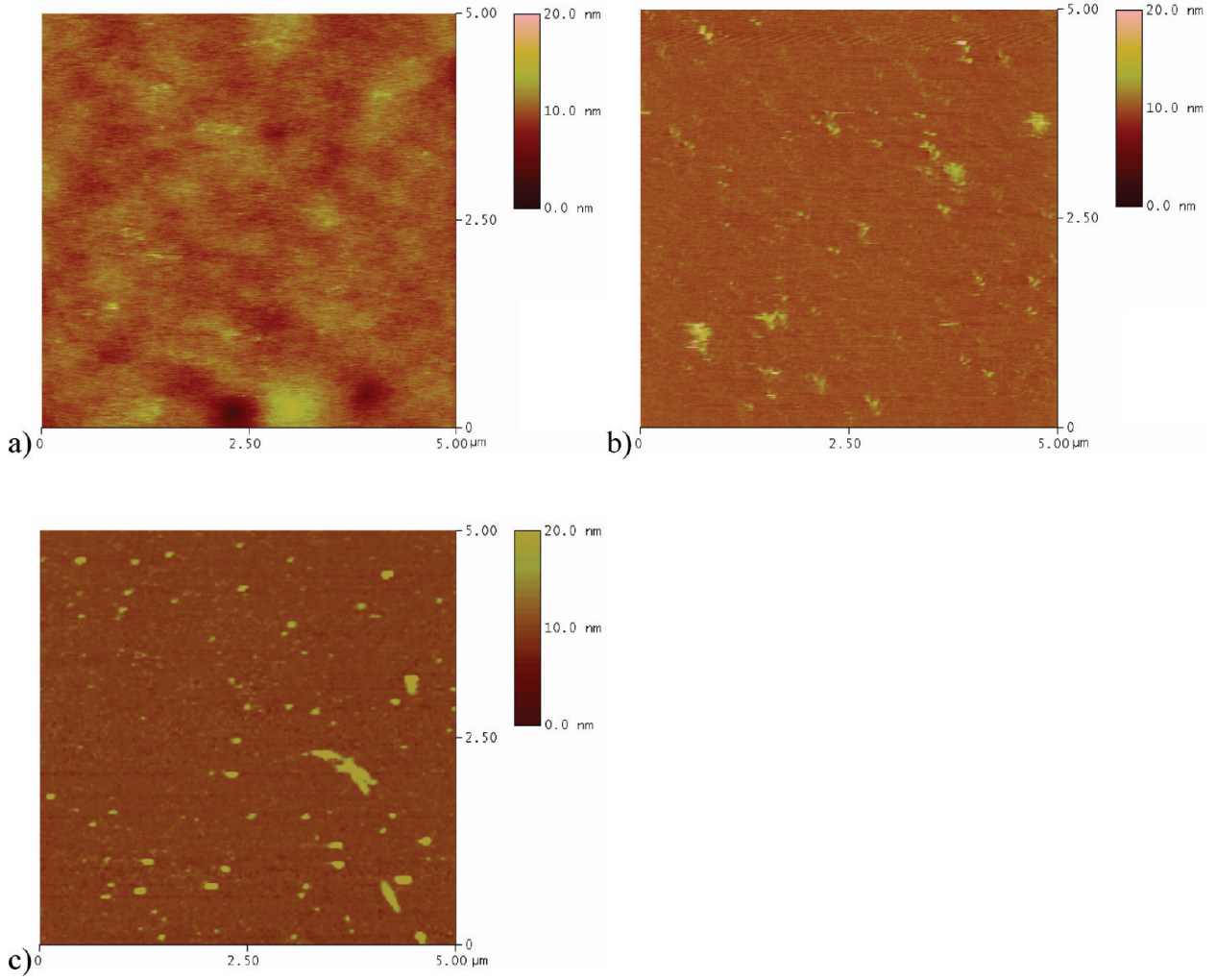

Figure 8. AFM images of a PAA layer with a grafting density of 0.15 chain/nm^2 exposed to (a) a pH 9 solution, (b) a 1×10^{-2} M NaCl pH 9 solution after 1 week, and (c) AFM image of a bare mica.

grafting density and salt concentration obtained by the least-squares fit is $L \propto \sigma^{1.09} C_s^{-0.17}$ (Figure 7b) with $R^2 = 0.95$. This behavior is different from the expected theoretical salted regime scaling law ($L \propto \sigma^{1/3} C_s^{-1/3}$). Interestingly, the effect of added salt is similar to previous experimental PMAA studies for $\sigma = 0.12$ chain/nm^2 ($M_n = 106$ kg/mol) that follow $L \propto C_s^{-0.24}$ at pH 6.[21] The increase in brush thickness with grafting density is considerably larger than that expected by scaling analysis for the salted regime ($L \propto \sigma^{0.33}$). An experimental PAA study has also shown a trend ($L \propto \sigma^{0.75}$) that is higher than the theoretical one for the salted brush regime.[20] Moreover, this experimental study reports an effect of added salt on brush thickness that is more pronounced for moderate to high grafting densities ($\sigma \geq 0.15$ chain/nm^2) than for low grafting density ($\sigma \sim 0.1$ chain/nm^2), whereas our data ($L \propto \sigma^{1.09} C_s^{-0.17}$) show a unique scaling relation for a large range of grafting densities. The $L \propto \sigma$ scaling behavior is usually predicted for quenched brushes (Pincus regime), low grafting density regimes, or low salt concentrations (weak screening effects).[19] Therefore, our results suggest that the dissociated PAA brushes at pH 9 do not collapse under electrostatic screening effects as much as theoretically predicted even at high added salt concentration (100 mM). This could partly explain the observed linear variation between L and σ that is otherwise predicted for weak screening effects.[19]

The swelling reversibility of PAA layers at pH 9 and at different ionic strengths was additionally investigated. Two samples with different grafting densities ($\sigma = 0.15$ and 0.49 chain/nm^2) were first exposed to pH 9 overnight in the absence of salt. The measured thickness was 97 ± 10 and 143 ± 8 nm, respectively (Figure 7a). They were then immersed in a pH 9 solution with added salt, and the thickness decreased to 63 ± 8 and 97 ± 4 nm, respectively. After thickness measurements, the samples were rinsed with Milli-Q water to remove a maximum amount of salt embedded in the brush, and they were then re-exposed to a salt-free pH 9 solution for two hours. The resulting measured brush thickness, 104 ± 10 and 124 ± 8 nm for σ of 0.15 and 0.49 chain/nm^2, respectively, were similar to the thickness measured at the same pH before immersion in salt. The swelling behavior of the brush is therefore reversible with pH and salt concentration and further confirms that the polymer is not hydrolyzed from the surface under these conditions. Moreover, the PAA layer ($\sigma = 0.15$ chain/nm^2) was stable for 2 days when immersed in a 1×10^{-2} M NaCl pH 9 solution as no significant changes in thickness ($\Delta L = 7 \pm 5$ nm) were measured. However, no thickness was measured after a week, and the observed surface topography was similar to that of a bare mica (Figure 8). Both observations suggest that the polymer layer is cleaved from the substrate. The presence of salt might induce slow ionization of the undissociated repeating units

close to the surface. This disrupts the protective layer of the immobilized initiator, exposing it to conditions that are known to hydrolyze the labile bond. The observed kinetics suggests that the hydrolysis reaction is slow and occurs over the course of several days. The PAA layer is therefore relatively stable under our experimental conditions and reliable correlations between polymer conformation and surface properties can be had.

Conclusions

The swelling behavior of irreversibly attached PAA brushes was studied for the first time on mica surfaces as a function of grafting density, pH, and salt concentration by AFM step-height measurements. The fully protonated PAA brushes behave like neutral brushes in a poor solvent regime, as they adopted a collapsed conformation regardless of both ionic strength and grafting density. Swelling occurs as a sharp transition, from collapsed to swollen conformation, with increasing pH as a result of monomer dissociation and a change in solvent strength. The dissociated PAA brushes in salt-free solution and at high pH behave like brushes in the Pincus regime, suggesting the presence of electrostatic repulsions inside the brush and a distribution of counterions extending outside the brush. In the salted regime, our data show a unique scaling relation, $L \propto \sigma^{1.09} C_s^{-0.17}$, for a large range of grafting densities and salt concentrations (C_s) which is indicative of a weak electrostatic screening effect. The reversible conformation changes observed in the present study prove a better control and understanding of polyelectrolyte brush behavior.

Acknowledgment. Financial support from the Natural Sciences and Engineering Research Council of Canada, Canada Foundation for Innovation, and the Fonds québécois de la recherche sur la nature et les technologies is greatly acknowledged. We thank Prof. R. E. Prud'homme for access to AFM measurements and Prof. C. Pellerin for access to IR measurements.

Supporting Information Available: Surface preparation and polymer hydrolysis. This material is available free of charge via the Internet at http://pubs.acs.org.

References and Notes

(1) Reiter, G.; Auroy, P.; Auvray, L. *Macromolecules* **1996**, *29*, 2150–2157.
(2) Reiter, G.; Khanna, R. *Langmuir* **2000**, *16*, 6351–6357.
(3) Epps, T. H.; DeLongchamp, D. M.; Fasolka, M. J.; Fischer, D. A.; Jablonski, E. L. *Langmuir* **2007**, *23*, 3355–3362.
(4) Dunlop, I. E.; Briscoe, W. H.; Titmuss, S.; Jacobs, R. M. J.; Osborne, V. L.; Edmondson, S.; Huck, W. T. S.; Klein, J. *J. Phys. Chem. B* **2009**, *113*, 3947–3956.
(5) Raviv, U.; Giasson, S.; Kampf, N.; Gohy, J.-F.; Jérôme, R.; Klein, J. *Nature* **2003**, *425*, 163–165.
(6) Zeng, H. B.; Tian, Y.; Zhao, B. X.; Tirrell, M.; Israelachvili, J. *Langmuir* **2009**, *25*, 4954–4964.
(7) Vyas, M. K.; Nandan, B.; Schneider, K.; Stamm, M. *J. Colloid Interface Sci.* **2008**, *328*, 58–66.
(8) Kobayashi, M.; Kaido, M.; Suzuki, A.; Ishihara, K.; Takahara, A. *J. Jpn. Soc. Tribol.* **2008**, *53*, 357–362.
(9) Drummond, C.; Rodriguez-Hernandez, J.; Lecommandoux, S.; Richetti, P. *J. Chem. Phys.* **2007**, *126*, 184906/1–12.
(10) Zdyrko, B.; Klep, V.; Li, X. W.; Kang, Q.; Minko, S.; Wen, X. J.; Luzinov, I. *Mater. Sci. Eng., C* **2009**, *29*, 680–684.
(11) De Giglio, E.; Cometa, S.; Cioffi, N.; Torsi, L.; Sabbatini, L. *Anal. Bioanal. Chem.* **2007**, *389*, 2055–2063.
(12) Hollmann, O.; Gutberlet, T.; Czeslik, C. *Langmuir* **2007**, *23*, 1347–1353.
(13) Xu, F. J.; Neoh, K. G.; Kang, E. T. *Prog. Polym. Sci.* **2009**, *34*, 719–761.
(14) Zhulina, E. B.; Birshtein, T. M.; Borisov, O. V. *Macromolecules* **1995**, *28*, 1491–1499.
(15) Israels, R.; Leermakers, F. A. M.; Fleer, G. J. *Macromolecules* **1994**, *27*, 3087–3093.
(16) Biesheuvel, P. M. *J. Colloid Interface Sci.* **2004**, *275*, 97–106.
(17) Israels, R.; Leermakers, F. A. M.; Fleer, G. J.; Zhulina, E. B. *Macromolecules* **1994**, *27*, 3249–3261.
(18) Pincus, P. *Macromolecules* **1991**, *24*, 2912–2919.
(19) Zhulina, E. B.; Klein Wolterink, J.; Borisov, O. V. *Macromolecules* **2000**, *33*, 4945–4953.
(20) Currie, E. P. K.; Sieval, A. B.; Fleer, G. J.; Cohen Stuart, M. A. *Langmuir* **2000**, *16*, 8324–8333.
(21) Parnell, A. J.; Martin, S. J.; Dang, C. C.; Geoghegan, M.; Jones, R. A. L.; Crook, C. J.; Howse, J. R.; Ryan, A. J. *Polymer* **2009**, *50*, 1005–1014.
(22) Liberelle, B.; Giasson, S. *Langmuir* **2008**, *24*, 1550–1559.
(23) Zhang, H. N.; Ruhe, J. *Macromolecules* **2005**, *38*, 4855–4860.
(24) Biesalski, M.; Johannsmann, D.; Rühe, J. *J. Chem. Phys.* **2002**, *117*, 4988–4994.
(25) Bendejacq, D.; Ponsinet, V.; Joanicot, M. *Eur. Phys. J. E* **2004**, *13*, 3–13.
(26) Wu, T.; Gong, P.; Szleifer, I.; Vlcek, P.; Subr, V.; Genzer, J. *Macromolecules* **2007**, *40*, 8756–8764.
(27) Lego, B.; François, M.; Skene, W. G.; Giasson, S. *Langmuir* **2009**, *25*, 5313–5321.
(28) Israelachvili, J.; Gee, M. L. *Langmuir* **1989**, *5*, 288–289.
(29) Horr, T. J.; Ralston, J.; Smart, R. S. C. *Colloids Surf., A* **1995**, *97*, 183–196.
(30) Liberelle, B.; Banquy, X.; Giasson, S. *Langmuir* **2008**, *24*, 3280–3288.
(31) Lego, B.; Skene, W. G.; Giasson, S. *Langmuir* **2008**, *24*, 379–382.
(32) *Polymer Handbook*, 4th ed.; Brandrup, J., Immergut, E. H., Grulke, E. A., Eds.; Wiley: New York, 1999.
(33) Ohno, K.; Morinaga, T.; Koh, K.; Tsujii, Y.; Fukuda, T. *Macromolecules* **2005**, *38*, 2137–2142.
(34) Tsujii, Y.; Ohno, K.; Yamamoto, S.; Goto, A.; Fukuda, T. *Adv. Polym. Sci.* **2006**, *197*, 1–45.
(35) Behling, R. E.; Williams, B. A.; Staade, B. L.; Wolf, L. M.; Cochran, E. W. *Macromolecules* **2009**, *42*, 1867–1872.
(36) Boyes, S. G.; Granville, A. M.; Mirous, B. K.; Akgun, B.; Brittain, W. J. *Polym. Prepr.* **2003**, *44*, 420–421.
(37) Matyjaszewski, K.; Miller, P. J.; Shukla, N.; Immaraporn, B.; Gelman, A.; Luokala, B. B.; Siclovan, T. M.; Kickelbick, G.; Vallant, T.; Hoffmann, H.; Pakula, T. *Macromolecules* **1999**, *32*, 8716–8724.
(38) Boyes, S. G.; Akgun, B.; Brittain, W. J.; Foster, M. D. *Macromolecules* **2003**, *36*, 9539–9548.
(39) Liberelle, B.; Giasson, S. *Langmuir* **2007**, *23*, 9263–9270.
(40) Asenath Smith, E.; Chen, W. *Langmuir* **2008**, *24*, 12405–12409.
(41) Ross, R. S.; Pincus, P. *Macromolecules* **1992**, *25*, 2177–2183.
(42) Carrillo, J.-M. Y.; Dobrynin, A. V. *Langmuir* **2009**, *25*, 13158–13168.
(43) Borisov, O. V.; Birshtein, T. M.; Zhulina, E. B. *J. Phys. II* **1991**, *1*, 521–526.
(44) Pryamitsyn, V. A.; Leermakers, F. A. M.; Fleer, G. J.; Zhulina, E. B. *Macromolecules* **1996**, *29*, 8260–8270.
(45) Sonnenberg, L.; Parvole, J.; Borisov, O.; Billon, L.; Gaub, H. E.; Seitz, M. *Macromolecules* **2006**, *39*, 281–288.
(46) Lide, D. R. *Handbook of Chemistry and Physics*, 87th ed.; CRC Press: Boca Raton, FL, 2006−2007.
(47) Arnold, R. *J. Colloid Sci.* **1957**, *12*, 549–556.
(48) Chen, K. M.; Jiang, X.; Kimerling, L. C.; Hammond, P. T. *Langmuir* **2000**, *16*, 7825–7834.
(49) Currie, E. P. K.; Sieval, A. B.; Avena, M.; Zuilhof, H.; Sudhölter, E. J. R.; Cohen Stuart, M. A. *Langmuir* **1999**, *15*, 7116–7118.
(50) Witte, K. N.; Kim, S.; Won, Y.-Y. *J. Phys. Chem. B* **2009**, *113*, 11076–11084.